Nonlinear cascaded quantum network with giant emitters

Citation for the original published paper (version of record):
Wang, X., Li, J., Wang, Z. et al (2026). Nonlinear cascaded quantum network with giant emitters. Communications Physics, 9(1). http://dx.doi.org/10.1038/s42005-026-02618-3

(article starts on next page)

communications physics
A Nature Portfolio journal

Article

https://doi.org/10.1038/s42005-026-02618-3

Nonlinear cascaded quantum network with giant emitters

Check for updates

Xin Wang [1,2] ✉, Jia-Qi Li [1], Zhihai Wang [3], Anton Frisk Kockum [4], Lei Du [4], Tao Liu [5] ✉ & Franco Nori [2,6]

Chiral quantum optics is central to developing scalable quantum networks, yet existing approaches rely predominantly on linear single-photon regimes. It remains unclear how to generate directional multiphotons. Here we show that giant emitters coupled to nonlinear quantum optical baths enable tunable directional correlated photons, revealing a mechanism for multiphoton directional emission. We demonstrate that the propagation phases of correlated photons, together with the coupling phases of giant emitters, can generate destructive interference in one direction while enhancing emission in the opposite direction, making directionality fully tunable. Building on this mechanism, we introduce a nonlinear cascaded quantum network paradigm mediated by "correlated flying qubits", providing a configurable building block enabling distinct many-body applications beyond linear unidirectional setups. These results reveal a rich landscape for engineering multiphoton propagation and correlations through interference in giant emitter-nonlinear bath architectures, offering pathways for quantum networks and strongly correlated light-matter platforms.

Chiral quantum optics, where light propagates in a preferred direction without back-scattering, is a prerequisite for communication protocols in a scalable cascaded quantum network[1–5]. Directional photons (serving as flying qubits) can connect remote nodes deterministically[6,7], and underpin unique applications beyond conventional bidirectional networks[8–12]. Recently, the nonlinear (multiphoton) regime of cascaded quantum systems has yielded many interesting proposals[13–15] for its potential to provide directional many-body resources in quantum communication, metrology, and sensing, with applications spanning from fundamental science to real-world technology[16–21]. For example, due to the interplay of nonlinearity and directional transport, many-body ordered states of light can be produced in a waveguide[22]. However, in conventional optical materials, the nonlinearity is ultraweak[23,24], and the unidirectional photons are usually uncorrelated. Therefore, constructing nonlinear cascaded quantum networks supporting scalable many-body quantum information processing remains a significant theoretical and experimental challenge, which has been little exploration.

Recent progress in engineered quantum platforms has opened promising pathways toward overcoming this challenge, such as superconducting circuit QED via the intrinsic anharmonicity[25–27] or Rydberg atom arrays via dipole blockade[28,29]. A notable example is provided by nonlinear waveguides, which are often modeled by Bose–Hubbard Hamiltonians with on-site photon–photon interactions[30–33]. In such systems, the interplay between nonlinearity and dispersion leads to strongly correlated multiphoton states, where photons can become bound together in real space[34–37]. These correlated states, in turn, can mediate super-correlated radiation dynamics and enable the generation of correlated photon pairs[38–42].

In parallel, the emerging paradigm of giant atoms has attracted considerable attention[43–47]. A giant atom couples to a photonic or phononic bath at multiple discrete points, with an effective size comparable to the operating wavelength[48–54]. This multi-point coupling structure gives rise to multiple decay channels that interfere quantum mechanically. By engineering the geometry and phase of these coupling points, one can tailor the interference to facilitate interesting phenomena such as decoherence-free dipole-dipole interactions[55–58], oscillating bound states[59–62], and chiral quantum effects[63–65].

In this work, we show that multiple giant emitters coupled to a nonlinear waveguide enable tunable multiphoton directional emission via interference, revealing a mechanism for the directional emission of strongly correlated photons. Our proposed setup can generate directionally correlated photon resources and serve as a building block for constructing nonlinear cascaded quantum networks mediated by "correlated flying

[1]Shaanxi Province Key Laboratory of Quantum Information and Quantum Optoelectronic Devices, School of Physics, Xi'an Jiaotong University, Xi'an, 710049, P. R. China. [2]Center for Quantum Computing, RIKEN, Wako-shi, Saitama, 351-0198, Japan. [3]Center for Quantum Sciences and School of Physics, Northeast Normal University, Changchun, 130024, P. R. China. [4]Department of Microtechnology and Nanoscience, Chalmers University of Technology, 41296 Gothenburg, Sweden. [5]School of Physics and Optoelectronics, South China University of Technology, Guangzhou, 510640, P. R. China. [6]Physics Department, The University of Michigan, Ann Arbor, MI, 48109-1040, USA. ✉e-mail: wangxin.phy@xjtu.edu.cn; liutao0716@scut.edu.cn

qubits". Furthermore, we demonstrate that this nonlinear network enables numerous many-body applications beyond the capabilities of linear chiral systems.

Results and discussion

Model

The nonlinear waveguide in our setup consists of an array of coupled nonlinear cavities, as depicted in Fig. 1a. In the frame rotating with the cavity frequency ω_c, the waveguide Hamiltonian is ($\hbar = 1$)

$$H_{\rm w} = \sum_n \left[\frac{U}{2} a_n^\dagger a_n^\dagger a_n a_n - J\left(a_n^\dagger a_{n+1} + {\rm H.c.}\right)\right], \tag{1}$$

where a_n ($a_n^\dagger$) is the photon annihilation (creation) operator of the nth cavity, J is the nearest-neighbor hopping rate, and U is the on-site photon-photon interaction strength. Throughout this work, we focus on systems with attractive interactions $U < 0$. A detailed discussion of the repulsive case $U > 0$ is provided in Supplementary Note 1 and Supplementary Note 2D.

Due to the nonlinear potential, strongly correlated photonic states exist in this waveguide. For example, a state called "doublon"[34,35], where two photons are bound together when propagating along the waveguide, emerges in the two-photon subspace. Within the center-of-mass and relative coordinates, i.e., $x_c = (n_1 + n_2)/2$ and $r_d = n_1 - n_2$, the doublon wave function can be expressed as $\Psi_K(x_c, r_d) = e^{iKx_c} u_K(r_d)$, with K the center-of-mass quasi-momentum. The eigen-equation is then derived as

$$E u_K(r_{\rm d}) = -2J\cos\left(\frac{K}{2}\right)\sum_{\pm} u_K(r_{\rm d} \pm 1) + U\delta_{r_{\rm d},0} u_K(r_{\rm d}), \tag{2}$$

Taking the nonlinear potential as the interaction terms $V(r_{\rm d}) = U\delta_{r_{\rm d},0}$, the full Green's function is obtained via the Lippmann–Schwinger equation[35]:

$$G_K(E, r_{\rm d}) = G_K^0(E, r_{\rm d}) + G_K^0(E, r_{\rm d})\frac{G_K^0(E, r_{\rm d}=0)U}{1 - G_K^0(E, r_{\rm d}=0)U}. \tag{3}$$

$G_K^0(E, r_{\rm d})$ denotes the unperturbed Green's function, which satisfies $(E - H_0)G_K^0(E, r_{\rm d}) = \delta_{r_{\rm d},0}$, with H_0 being the unperturbed Hamiltonian without nonlinear terms. Here, we focus on the doublon state, arising from the nonlinear potential U. To identify such a bound state, we require

$$1 - G_K^0(E, r_{\rm d}=0)U = 0. \tag{4}$$

which implies the contribution of the first term in Eq. (3), corresponding to scattering states and the eigensolution of H_0, can be neglected. By solving Eq. (4), the dispersion relation of the doublon state is derived (see Fig. 1c)

$$E_K = -\sqrt{U^2 + 16J^2\cos^2(K/2)}. \tag{5}$$

The corresponding relative wave function is given by

$$u_K(r_{\rm d}) = u_0 \exp\left[-\frac{|r_{\rm d}|}{L_u(K)}\right], \tag{6}$$

where $L_u^{-1}(K) = {\rm asinh}\left[U/4J\cos(K/2)\right]$ is the inverse decay length of the two-photon correlation in space, and u_0 is a normalization factor. Note that $L_u(K)$ decreases rapidly as the interaction strength U increases. This indicates that, in the presence of the nonlinear potential U, the two photons are tightly bound within a spatial length L_u, when propagating along the waveguide. For further details on the derivation, we refer the interested reader to ref. 35 and the Supplementary Note 1.

We consider $\mathcal{N}$ GEs interacting with the waveguide. The two coupling points of GE m are located at $n_m^{l(r)}$ (see Fig. 1a). The system Hamiltonian is

$$H = H_{\rm w} + \sum_{m=1}^{\mathcal{N}}\left[\frac{\Delta_e}{2}\sigma_m^z + g\sum_{\tau={\rm l,r}}\left(e^{i\phi_m^\tau}\sigma_m^- a_{n_m^\tau}^\dagger + {\rm H.c.}\right)\right], \tag{7}$$

with $\Delta_e = \omega_e - \omega_c$ (ω_e is the emitter frequency), g the coupling strength at each coupling point, σ^z a Pauli matrix, and σ_- the lowering operator. A local phase $\phi_m^{l(r)}$ is assumed at each coupling point. We first take a giant-emitter pair (GEP), i.e., $\mathcal{N} = 2$, as an example. The size of emitter m is $d = |n_m^{\rm l} - n_m^{\rm r}|$ and the distance between the centers of the two emitters is $D = (|n_2^{\rm l} + n_2^{\rm r}| - |n_1^{\rm l} + n_1^{\rm r}|)/2$. When Δ_e is significantly gapped from scattering states, i.e., $\Delta_e < -2J$, emission of a single photon is suppressed. We set $2\Delta_e$ lying inside the doublon spectrum (see Fig. 1b) such that the GEP will emit correlated photons, i.e., doublons[38].

We assume that, initially, the two emitters are in their excited states and the waveguide is in its vacuum state. Since the Hamiltonian in Eq. (7) conserves the total excitation number, the system state is

$$\begin{aligned}|\psi(t)\rangle = \Big[&c_e(t)\sigma_1^+\sigma_2^+ + \sum_K c_K(t)\mathcal{D}_K^\dagger \\ &+ \sum_{m=1,2}\sum_k c_{mk}\sigma_m^+ a_k^\dagger\Big]|g, g, {\rm vac}\rangle,\end{aligned} \tag{8}$$

where $c_e(t)$ [$c_K(t)$] is the probability amplitude for the GEP (doublon mode K) being excited, $\mathcal{D}_K^\dagger$ is the creation operator of doublon mode K, $a_k^\dagger = 1/\sqrt{N}\sum_n e^{ikn}a_n^\dagger$ are the photonic operators in momentum space, and $|c_{mk}|^2$ is the probability for both the mth giant emitter and the single-photon mode k being excited. Given that $g \ll |\Delta_e - 2J|$, we can adiabatically eliminate the single-photon intermediate states c_{mk} by assuming $i\dot{c}_{mk}(t) = 0$. The evolution of $c_e(t)$ and $c_K(t)$ is then given by (see Supplementary Note 2 A for a detailed discussion)

$$i\dot{c}_e(t) = -\frac{g^2}{J\sqrt{N}}\sum_K F_K^* c_K(t), \tag{9}$$

$$i\dot{c}_K(t) = \Delta_K c_K(t) - \frac{g^2}{J\sqrt{N}} F_K c_e(t), \tag{10}$$

where $\Delta_K = E_K - 2\Delta_e$. F_K is expressed as a sum over four decay channels:

$$F_K = \sum_{\tau,\sigma}\vec{e}_{\tau\sigma}(K), \tag{11}$$

where each channel is represented as a complex vector to facilitate the interpretation of interference effects. Each vector is defined as

$$\vec{e}_{\tau\sigma}(K) = A_K\left(r_d^{\tau\sigma}\right)e^{i\phi_1^\tau}e^{i\phi_2^\sigma}e^{-iKx_c^{\tau\sigma}}, \tag{12}$$

with the amplitude

$$A_K\left(r_d^{\tau\sigma}\right) = \sum_k \cos\left[(k - K/2)r_d^{\tau\sigma}\right]L_{k,K},$$
$$L_{k,K} = \frac{2\sqrt{2}J}{N(\omega_k - \Delta_e)}\sum_m e^{-i(k-K/2)m}u_K(m),$$

where $x_c^{\tau\sigma} = (n_1^\tau + n_2^\sigma)/2$, $r_d^{\tau\sigma} = n_1^\tau - n_2^\sigma$, $\delta_k = \omega_k - \Delta_e$ and $\omega_k = -2J\cos(k)$ is the single-photon dispersion relation. Taking $\vec{e}_{\rm lr}$ schematically depicted in Fig. 2a as an example, we see that this correlation function represents dual processes: emitter 1 (2) excites a single-photon intermediate state spreading around the point $n_1^{\rm l}$ ($n_2^{\rm r}$) with an encoded phase $\phi_1^{\rm l}$ ($\phi_2^{\rm r}$). Meanwhile, emitter 2 (1) emits a single photon at point $n_2^{\rm r}$ ($n_1^{\rm l}$) with encoded phase $\phi_2^{\rm r}$ ($\phi_1^{\rm l}$). The overlap between the wave functions of these photon pairs and the doublon state K is proportional to $\vec{e}_{\rm lr}$ (see Supplementary Note 2B).

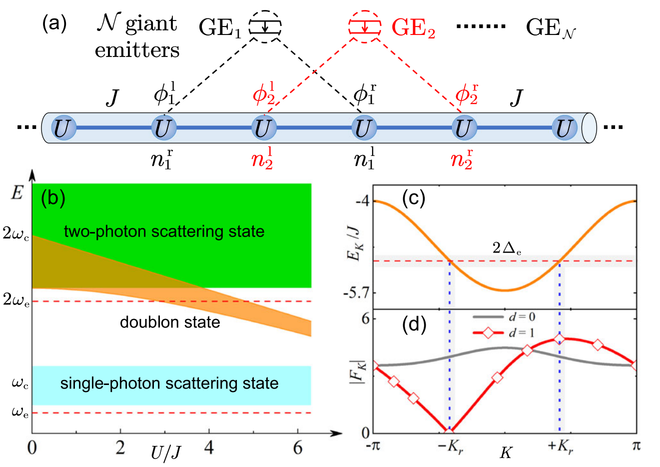

Fig. 1 | Interactions between giant emitters and correlated photons. **a** Sketch of $\mathcal{N}$ giant emitters (GEs) coupled to a nonlinear waveguide (a coupled-cavity array with hopping rates J and on-site nonlinear potentials U). Giant emitter m couples to the waveguide at $n_m^{l(r)}$ with phases $\phi_m^{l(r)}$. The emitter size is $d = |n_m^{\rm r} - n_m^{\rm l}|$; the emitter centers are separated by a distance D. **b** Waveguide spectrum as a function of U. The lower (upper) red dashed line marks the GE (giant-emitter pair, GEP) frequency ω_e ($2\omega_e$). **c** Doublon dispersion relation E_K. The red dashed curve denotes the frequency $2\Delta_e$. **d** Effective coupling strength $|F_K|$ as a function of doublon wave vector K for different d. When $d = 1$, K_r is the optimal unidirectional point. Two blue dashed curves denote the resonance mode $\pm K_r$. Parameters: $D = 0$, $\Phi_{1,2}^{\rm e} = \phi_{1,2}^{\rm r} - \phi_{1,2}^{\rm l} = \pi/2$, and $U = 4J$.

After adiabatically eliminating the single-photon intermediate state, we obtain the reduced two-photon state

$$|\psi(t)\rangle = \left[c_{\rm e}(t)\sigma_1^+\sigma_2^+ + \sum_K c_K(t)\mathcal{D}_K^\dagger\right]|g, g, {\rm vac}\rangle. \tag{13}$$

From Eqs. (9) and (10), the effective interaction Hamiltonian between the GEP and the nonlinear waveguide, i.e., the state $|e, e, {\rm vac}\rangle$ and $|g, g, K\rangle$ can be further derived as

$$H_{\rm int} = \frac{g^2}{J}\sum_{\tau,\sigma}\sigma_1^-\sigma_2^-\mathcal{D}_{n_1^\tau,n_2^\sigma}^\dagger + {\rm H.c.}, \tag{14}$$

$$\mathcal{D}_{n_1^\tau,n_2^\sigma}^\dagger = \frac{1}{\sqrt{N_c}}\sum_K e^{i\Delta_K t}F_K\mathcal{D}_K^\dagger. \tag{15}$$

Note that, the operator $\mathcal{D}_{n_1^\tau,n_2^\sigma}^\dagger$ is defined in the interaction picture, which contains a time-dependent phase factor.

Interference-induced supercorrelated directional emission

We assume that the effective coupling strength g^2F_K/J is sufficiently weak compared to the doublon bandwidth that the Born–Markov approximation holds[66]. The supercorrelated decay of the GEP then becomes

$$c_{\rm e}(t) = \exp\left(-\frac{\Gamma_+ + \Gamma_-}{2}t\right),\ \Gamma_\pm = \frac{g^4}{v_g J^2}\left|F_{\pm K_r}\right|^2, \tag{16}$$

where $E_{K_r} = 2\Delta_{\rm e}$, $v_{\rm g} = (\partial E_K/\partial K)|_{K=K_r}$ is the group velocity, and Γ_+ (Γ_-) denotes the supercorrelated emission rate to the right (left). Figure 1d shows $|F_K|$ as a function of K for different d. When $d = 0$, the emitters are small and $|F_K| = |F_{-K}|$ always, regardless of $\phi_{1,2}^{\rm r,l}$, so there is no directional emission. However, for GEs with $d \neq 0$ and $\Phi_{1,2}^{\rm e} \neq 0$, directional emission of correlated photon pairs emerges. These rates define the chiral factor $C = (\Gamma_+ - \Gamma_-)/(\Gamma_+ + \Gamma_-)$.

Setting $d = 1$, $D = 0$, and $\Phi_{1,2}^{\rm e} = \phi_{1,2}^{\rm r} - \phi_{1,2}^{\rm l} = \pi/2$, we plot the waveguide field distribution and the evolution of $|c_{\rm e}(t)|^2$ in Fig. 2b, c. The numerically calculated evolution is an exponential decay, in excellent agreement with analytical results. Due to the local nonlinear potential, the two photons are strongly bunched; the spatial correlation function $\mathcal{G}^{(2)}(r_{\rm d})$ has its maximum at $r_{\rm d} = 0$. Most strikingly, the emission of this correlated photon pair exhibits a strong preference for a certain direction, as shown in Fig. 2b.

Increasing D (fixing d), the chiral factor changes little, while the decay rate quickly decreases to zero. The ordering of the coupling points has no significant effect on the directional emission[55]. Details on the effect of varying D and d are given in Supplementary Note 2 C. Figure 2d plots C as a function of the phases $\Phi_{1,2}^{\rm e}$, showing that a large chiral factor is robust to relatively large imprecision in $\Phi_{1,2}^{\rm e}$ and that C is smoothly tuned in the full range $C \in (-1, 1)$ by changing $\Phi_{1,2}^{\rm e}$. These key results indicate that the proposed setup may serve well as a source for directionally correlated photons.

To better understand the mechanism for directional emission, we depict the four supercorrelated decay channels $\vec{e}_{\tau\sigma}$ in Fig. 3a–d, with orange dots denoting single photons emitted from distinct emitters and stars being the centers-of-mass of correlated photon pairs. The phase of $\vec{e}_{\tau\sigma}$ consists of the local phases $\phi_1^\tau + \phi_2^\sigma$ and the accumulated propagation phase $\Phi_{\rm d} = -K_r x_{\rm c}^{\tau\sigma}$ associated with the center-of-mass $x_{\rm c}^{\tau\sigma}$ of the correlated photon pair (not the single-photon propagation phase). Taking $n_1^{\rm l} = 0$ as the origin, and considering the scenario where two giant emitters couple to the same locations, i.e., $n_1^{\rm l} = n_2^{\rm l}$ and $n_1^{\rm r} = n_2^{\rm r}$, the four decay channels are simplified as

$$\begin{aligned}
\vec{e}_{\rm ll} &= A_{\rm ll}e^{i\phi_1^{\rm l}}e^{i\phi_2^{\rm l}} = A_{\rm ll}e^{i\Phi_0},\\
\vec{e}_{\rm lr} &= A_{\rm lr}e^{i\phi_1^{\rm l}}e^{i\phi_2^{\rm r}}e^{-iK\frac{d}{2}} = A_{\rm lr}e^{i\Phi_0}e^{i\Phi_2^{\rm e}}e^{-iK\frac{d}{2}},\\
\vec{e}_{\rm rl} &= A_{\rm rl}e^{i\phi_1^{\rm r}}e^{i\phi_2^{\rm l}}e^{-iK\frac{d}{2}} = A_{\rm rl}e^{i\Phi_0}e^{i\Phi_1^{\rm e}}e^{-iK\frac{d}{2}},\\
\vec{e}_{\rm rr} &= A_{\rm rr}e^{i\phi_1^{\rm r}}e^{i\phi_2^{\rm r}}e^{-iKd} = A_{\rm rr}e^{i\Phi_0}e^{i\Phi_1^{\rm e}}e^{i\Phi_2^{\rm e}}e^{-iKd},
\end{aligned}$$

where $\Phi_0 = \phi_1^{\rm l} + \phi_2^{\rm l}$ is the global reference phase, which does not affect the dynamics. The interference is solely determined by the phase difference between the two coupling points of each giant emitter, i.e., $\Phi_1^{\rm e} = \phi_1^{\rm r} - \phi_1^{\rm l}$ ($\Phi_2^{\rm e} = \phi_2^{\rm r} - \phi_2^{\rm l}$). With $n_1^{\rm l} = n_2^{\rm l} = 0$ as the reference point, the propagation phases for the channels are ll $\to \Phi_{\rm d} = 0$, lr, rl $\to \Phi_{\rm d} = K_r d/2$, and rr $\to \Phi_{\rm d} = K_r d$. The interferences are illustrated in Fig. 3e, f for $\pm K_r$, respectively. At the optimal point $2\Delta_{\rm e} = E_{K_r}$, the interferences for the left- and right-propagating modes become asymmetric: the four vectors for $-K_r$ form a closed loop, i.e.,

$$|\sum_{\tau\sigma}\vec{e}_{\tau\sigma}(+K_r)| \gg |\sum_{\tau\sigma}\vec{e}_{\tau\sigma}(-K_r)| = 0.$$

The interaction between the GEP and the left-propagating mode vanishes (see Fig. 1d), and the GEP only emits correlated photons into the right direction, yielding $C \simeq 1$. When $2\Delta_{\rm e}$ is biased away from the optimal point, C decreases, as indicated in Fig. 2d. In the white region where $C = 0$, the GEP dynamics recover the small-atom behavior with non-directional emission[38]. The specific parameter regimes corresponding to $C = 0$ are discussed in Supplementary Note 2C. Moreover, the effects of emitter frequency mismatch are discussed in Supplementary Note 2D.

Note that our examples are the simplest giant emitters with two coupling points. For GEPs with $\mathcal{M}$ coupling points per emitter, there are $\mathcal{M}^2$ supercorrelated decay channels interfering with each other, which is much more complicated than single-photon interference in one giant atom[43,53,67]. When $\mathcal{M} \geq 3$, realizing broadband directional emission for doublons is possible by considering optimal methods[68].

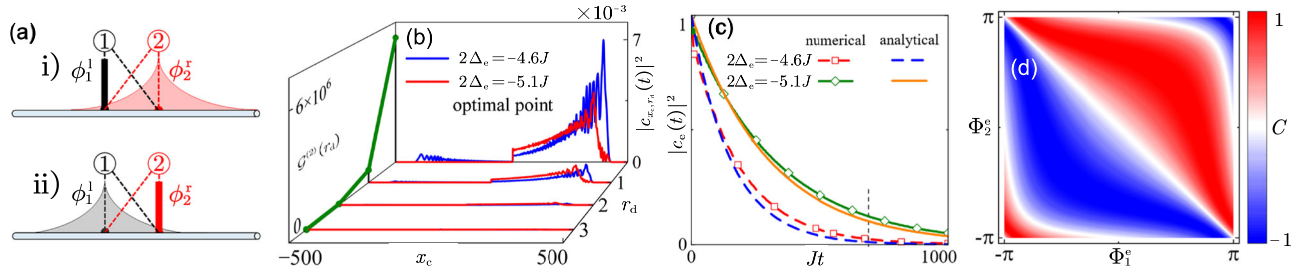

Fig. 2 | Directional emission of doublons. a Sketches of the dual transition processes described by $\vec{e}_{lr}$. Vertical bars indicate a single photon localized at n_1^l (n_2^r), while the shaded curves represent the spatial envelope of the intermediate single-photon state. Two giant emitters {①, ②} are coupled to the waveguide at positions marked by the black and red dashed arrows, respectively. **b** Two-photon joint probability distribution $|c_{x_c,r_d}(t)|^2$ at time $Jt = 600$ [dashed line in (**c**)] with $2\Delta_e = -5.1J$ (optimal emission point). $x_c = (n_1 + n_2)/2$ and $r_d = n_1 - n_2$ denote the center-of-mass and relative coordinates of two photons at sites n_1 and n_2. The two-point correlation function $\mathcal{G}^{(2)}(r_d)$ is also shown. **c** Time evolution of $|c_e(t)|^2$ for $2\Delta_e = -4.6J$ and $-5.1J$. **d** Chiral factor as a function of $\Phi_{1,2}^e = \phi_{1,2}^r - \phi_{1,2}^l$, with $2\Delta_K = -5.1J$. The coupling strength is set to $g = 0.1J$; other parameters are the same as in Fig. 1d.

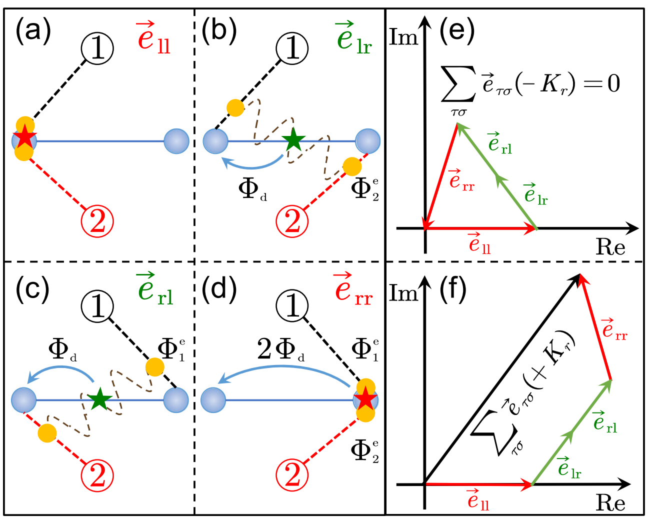

Fig. 3 | Interferences between different decay channels. a–d Sketches of the four decay channels $\vec{e}_{\tau\sigma}$ (τ, σ = l, r) of a GEP releasing two correlated photons into the waveguide. Orange dots represent single photons emitted from individual emitters, while stars denote centers of mass x_c of the correlated photon pairs. **e, f** Summation of $\vec{e}_{\tau\sigma}$ at the optimal point $\pm K_r$ for right- (left-) propagating modes.

Nonlinear cascaded quantum network

Analogously to conventional unidirectional quantum setups with uncorrelated single photons, a cascaded system is naturally formed when considering multiple nodes unidirectionally interacting with the same waveguide. Contrasting linear setups, such as interacting emitter pairs[6,7], multi-level atoms[69], and superradiance of atom ensembles (time-Dicke states)[70], our proposal utilizes super-correlated photons as "flying qubits", enhancing numerous many-body applications.

Figure 4a depicts a minimal example setup with two separate GEPs, A and B, interacting with a common waveguide. We assume that the two GEPs have the same geometric layout but are separated by a distance D_q, with D_q sufficiently larger than $L_u(K_r)$. This ensures that supercorrelated emission between emitters in different pairs, i.e., the process $\langle \mathrm{vac}|\mathcal{D}_K^\dagger \sigma_{A,1/2}^- \sigma_{B,1/2}^-|\mathrm{vac}\rangle$, is suppressed. The operator $\sigma_{\alpha,i}^-$ denotes the lowering operator of emitter α_i. Under this condition, we consider the initial state:

$$|\psi(t=0)\rangle = \sigma_{A,1}^+\sigma_{A,2}^+|g,g,\mathrm{vac}\rangle,$$

which only GEP A is excited, and states $\sigma_{A,1/2}^-\sigma_{B,1/2}^-|g,g,\mathrm{vac}\rangle$ can be neglected. Accordingly, the reduced system state analogous to (13) becomes:

$$|\psi(t)\rangle = \left[\sum_\alpha c_e^\alpha(t)\sigma_{\alpha,1}^+\sigma_{\alpha,2}^+ + \sum_K c_K(t)\mathcal{D}_K^\dagger\right]|g,g,\mathrm{vac}\rangle. \tag{17}$$

Here, α = A, B denotes that supercorrelated radiation is confined within individual GEPs. Analogous to Eq. (14), the interaction Hamiltonian can be expanded in the basis of Eq. (17) as

$$H_{\mathrm{int}} = \frac{g^2}{J}\sum_\alpha\sum_{\tau,\sigma}\sigma_{\alpha,1}^-\sigma_{\alpha,2}^-\mathcal{D}^\dagger_{n_{\alpha,1}^\tau,n_{\alpha,2}^\sigma} + \mathrm{H.c.} \tag{18}$$

In contrast to Eq. (14), the labels now include an additional index α = A, B, where (α, i, τ) denotes the ith emitter in pair α coupled to the waveguide at position $n_{\alpha,i}^\tau$.

Consequently, the interaction Hamiltonian is simplified as

$$H_{\mathrm{int}} = \sum_{\alpha=A,B}\sum_K \frac{g_\alpha^2 e^{i\Delta_K t}}{J\sqrt{N}}F_{K,\alpha}\mathcal{D}_k^\dagger S_\alpha^- + \mathrm{H.c.}, \tag{19}$$

where $S_\alpha^- = \sigma_{\alpha,1}^-\sigma_{\alpha,2}^-$ is the joint-quantum-jump operator for GEP α and $F_{K,\alpha}$ is the correlation functions of GEP α [see Eq. (11)]. The individual supercorrelated decay rates for the two GEPs are $\Gamma_\pm^\alpha = |g_\alpha|^4/(v_g J^2)|F_{\alpha,\pm K_r}|^2$ (α = A, B), where +(−) represents propagation to the right (left). It naturally corresponds to a nonlinear master equation with joint-quantum-jump processes. Given that each GEP unidirectionally couples to the waveguide with $\Gamma_+^\alpha \gg \Gamma_-^\alpha$, a correlated photon pair (flying qubits) is unidirectionally radiated by GEP A, subsequently transferred along the waveguide, and absorbed by GEP B without information backflow, which forms a nonlinear cascaded quantum network. The numerical example can be seen in Supplementary Note 2F, and an application (steady four-partite entangled states between remote GEPs) can be seen in Supplementary Note 3A.

We now demonstrate a high-fidelity process for entangled-state transfer between two remote quantum nodes by modulating the decay rates of two GEPs. The modulation pulses are (see Supplementary Note 3B)

$$\Gamma_+^A(t) = \Gamma_+^B(\tau_D - t) = \frac{\exp(-ct^2)}{\frac{1}{\Gamma_0} - \sqrt{\frac{\pi}{4c}}\mathrm{erf}\left(t\sqrt{c}\right)}, \tag{20}$$

where $c = 1.01\times\Gamma_0^2\pi/2$, with Γ_0 the decay rate of GEP A at t = 0, and $\tau_D = D_q/v_g$ is the propagation time from A to B. The modulation pulses in

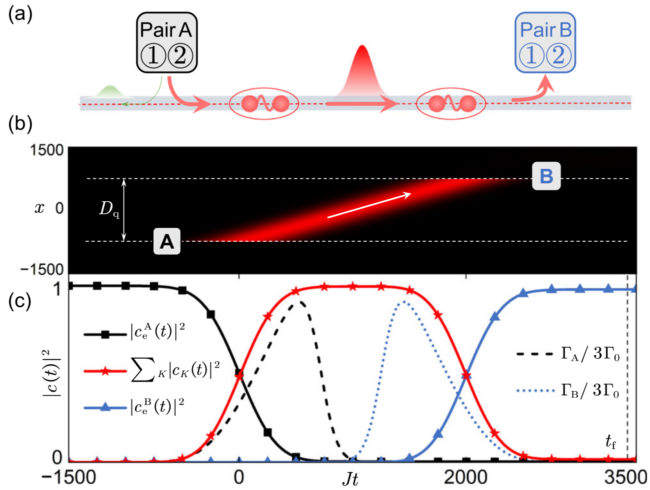

Fig. 4 | State transfer process mediated by directionally correlated photons. **a** Sketch of the nonlinear cascaded quantum system, where correlated photon pairs are unidirectionally emitted by GEP A and subsequently absorbed by GEP B without back-scattering. **b** The evolution of two-photon field distribution at $r_d = 0$ and **c** populations for the GEP A (black solid curve with squares), GEP B (blue solid curve with triangles), and doublon (red solid curve with stars) during the two-photon transfer process. The dashed lines in **b** mark the positions of GEP A and B, which are separated by a distance $D_q = 1.5 \times 10^3$. The modulations of the couplings are given by Eq. (20). The black dashed curve and blue dotted curve denote the modulation pulses of GEP A and B, respectively. Same parameters as in Fig. 2.

(20) minimize irreversible quantum jump processes and tailor the wavepacket of the correlated photons with time-reversal symmetry. Therefore, GEP B will perfectly absorb two correlated photons emitted by GEP A[1,8,9]. Because $\Gamma_+^\alpha(t) \propto |g_\alpha|^4$ in our proposal [cf. (16)], the modulated decay rates can be exactly mapped to time-dependent interactions $g_{A,B}(t)$. We numerically simulate two-excitation transfer between two GEPs in Fig. 4b,c. Given that the decay rates are modulated according to Eq. (20), the dark-state conditions hold in this nonlinear cascaded system, and the correlated two-photon field is trapped between the two GEPs without leaking outside. At the final time t_f, one finds that $\{|c_e^A(t_f)|^2, \sum_K |c_K(t_f)|^2\} \simeq 0$, and the absorption efficiency is $|c_e^B(t_f)|^2 \simeq 98\%$. This value is primarily limited by the intermediate single-photon process and the finite transfer time[9]. Reducing the coupling strength during state transfer suppresses the intermediate single-photon amplitudes, thereby improving the corresponding fidelity. However, it also reduces the doublon emission rate, leading to a longer transfer time. This not only slows down the quantum information protocol but also enhances the impact of other decoherence channels. Consequently, in a realistic experimental implementation, an optimal coupling strength $g(t)$ might be chosen to balance transfer fidelity with operation speed.

In linear waveguide QED setups, a single multi-level emitter can be adiabatically reduced to a single effective qubit for correlated-photon emission[69]. Since such a node lacks internal multipartite structure, it cannot support the direct transfer of many-body entangled states (e.g., GHZ states) between distant nodes. Moreover, unlike conventional GHZ-state distribution in linear waveguides[71], which requires sequential single-photon transmissions and numerous local operations, our nonlinear cascaded interface accomplishes this many-body task without the need for sequential control or post-processing. For example, an initial entangled state of GEP A, $|\Psi_A(t_0)\rangle = c_e^A|e,e\rangle + c_g^A|g,g\rangle$, can be directly mapped onto GEP B as $|\Psi_B(t_0)\rangle = c_e^B|e,e\rangle + c_g^B|g,g\rangle$ in a single-step operation.

States beyond doublons with $\mathcal{N}$ correlated photons, e.g., triplons, also exist in this nonlinear setup[72,73]. For example, the energy spectrum of the waveguide in the three-photon subspace is shown in Fig. 5a. There, three-photon bound states, referred to as "triplons", emerge between two- and three-photon scattering states. Those $\mathcal{N}$ correlated photons can also be unidirectionally routed among GEs by exploiting interference. We demonstrate this by considering three excited GEs coupling to the waveguide with identical phase differences Φ_t^e. Figure 5b shows that the three-photon field $|\Psi(r_1, r_2, r_3)|^2$ is unidirectionally emitted and strongly bunched at the diagonal positions. The joint-quantum-jump operator of this correlated process is $S_\alpha^- = \sigma_{\alpha1}^-\sigma_{\alpha2}^-\sigma_{\alpha3}^-$. The chiral factor also varies in the full range by changing Φ_t^e (see Fig. 5c).

We further consider an application in which the three GEs in two remote nodes are pumped via three-photon parametric down-conversion processes, i.e., $H_{\text{pump}} = \Omega_d \sum_{\alpha=A,B}(\mathcal{S}_\alpha^- + \mathcal{S}_\alpha^+)$. Such a nonlinear pump has been realized, for example, in circuit-QED platforms[74]. The dark state for this driven-dissipative cascaded system is (see Supplementary Note 4)

$$|\psi_0\rangle = |g\rangle^{\otimes 2\mathcal{N}} + i\frac{2\sqrt{2}\Omega_d}{\Gamma_+^\alpha}|S\rangle, \tag{21}$$

$$|S\rangle = \frac{|g\rangle^{\otimes\mathcal{N}} \otimes |e\rangle^{\otimes\mathcal{N}} - |e\rangle^{\otimes\mathcal{N}} \otimes |g\rangle^{\otimes\mathcal{N}}}{\sqrt{2}}, \tag{22}$$

with $\mathcal{N} = 3$ for triplons. In the limit $\Omega_d \gg \Gamma_+^\alpha$, the dark state is approximately $|\psi_0\rangle \simeq |S\rangle$, which is a six-partite maximally entangled state for two remote nodes. In Fig. 5c, we numerically show that the trapping fidelity F_{ψ_0} strongly depends on the chiral factor. In an ideal nonlinear cascaded network with $C \simeq 1$, the trapping fidelity can reach as high as $F_{\psi_0} \simeq 1$. When this nonlinear system transitions to a bidirectional configuration, F_{ψ_0} decreases accordingly.

Furthermore, we infer that groups of $\mathcal{N}$-photon states in nonlinear waveguides can serve as directional "correlated flying qubits". Figure 5d schematically depicts a cascaded quantum network where $\mathcal{N}$ GEs serve as quantum nodes, whose joint-quantum-jump operators are $\mathcal{S}_\alpha^- = \prod_j^{\mathcal{N}} \sigma_{\alpha j}^-$. Analogously, the cascaded master equation is

$$\dot{\rho} = -i\left(H_{\text{eff}}\rho - H_{\text{eff}}^\dagger\rho\right) + \mathcal{L}\rho\mathcal{L}^\dagger, \tag{23}$$

$$H_{\text{eff}} = -i\sum_\alpha \frac{\Gamma_+^\alpha}{2}\mathcal{S}_\alpha^+\mathcal{S}_\alpha^- - i\sum_{\alpha\beta}^{\beta>\alpha}\sqrt{\Gamma_+^\alpha\Gamma_+^\beta}\mathcal{S}_\beta^+\mathcal{S}_\alpha^-, \tag{24}$$

where $\mathcal{L} = \sum_\alpha \sqrt{\Gamma_+^\alpha}\mathcal{S}_\alpha^-$. Following the methods in Fig. 4, our proposal enables single-step transfer of an arbitrary $\mathcal{N}$-qubit GHZ state, $|\psi_0\rangle = c_e|e\rangle^{\otimes\mathcal{N}} + c_g|g\rangle^{\otimes\mathcal{N}}$, between two $\mathcal{N}$-body nodes, without decomposing it into sequential single-excitation processes. In summary, our work demonstrates that nonlinear waveguides can be configured as multiphoton buses supporting advanced many-body quantum applications.

Feasible implementation

Our proposal is feasible in circuit-QED systems[27,75,76]. An array of coupled transmon qubits[25] can be configured as the nonlinear waveguide. The hopping rate and Kerr nonlinearity of such an array demonstrated in experiments[30,77–79] are on the order of $J/2\pi \sim 50$ MHz and $U/2\pi \sim 200$ MHz, respectively.

The giant-atom configuration, with multiple discrete coupling points to a waveguide, has already been experimentally realized[52,56]. In our scheme, the relative coupling phases required for directional emission can be dynamically tuned via parametric modulation[65]. The transmon anharmonicity $U_{\text{giant}}/2\pi \sim 300$ MHz supports the two-level approximation for the emitters. Furthermore, time-dependent interactions between superconducting giant atoms and the nonlinear waveguide can be realized using the methods[65,80], achieving a coupling strength of $g/2\pi = 0.1J/2\pi \sim 5$ MHz.

Under these parameters, the supercorrelated emission rate is estimated as $\Gamma_\pm/2\pi \sim 1$ MHz (see Supplementary Note 3A), which is much larger than the intrinsic decoherence rate of a circuit-QED platform[81,82]. Therefore, the

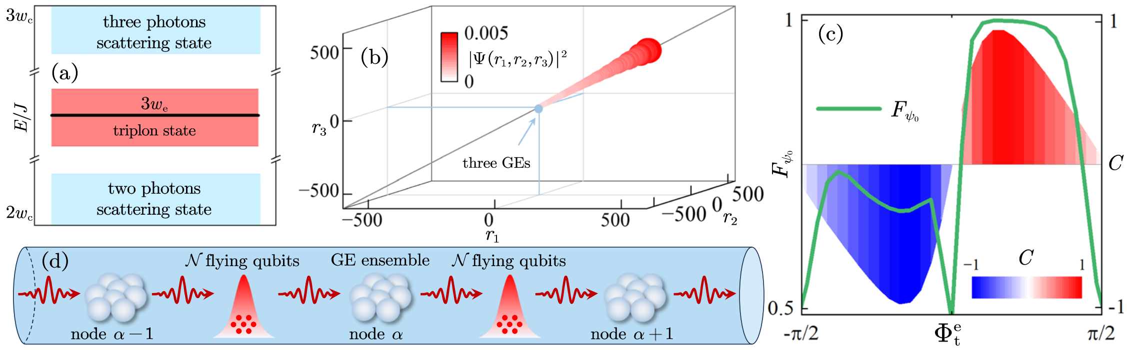

Fig. 5 | Nonlinear cascaded quantum network for many-body applications. a The total frequency of three GEs $3\omega_e$ (the black solid line) is set to be within the triplon spectrum. **b** Field distribution $|\Psi(r_1, r_2, r_3)|^2$ (mapped as bubble color and size) for triplons emitted from three GEs by setting $\Phi_t^e = 0.18\pi$. **c** The chiral factor C and the trapping fidelity F_{ψ_0} (green solid curve) for the state in Eq. (21) as functions of the phase difference Φ_t^e. **d** Sketch of a nonlinear cascaded quantum system, whose nodes are unidirectionally connected by $\mathcal{N}$ correlated photons. Here we set $3\Delta_e = -12.7J$ (inside the triplon spectrum). Other parameters are the same as in Fig. 2.

phenomena predicted in this work are possible to observe in current circuit-QED setups.

Conclusions

We show how to realize unidirectional transport of strongly correlated photons in a nonlinear waveguide interacting with GEs. Compared to the single-photon case, the interference channels are more complicated. The propagating phase related to the center of mass of correlated photons plays a crucial role in interference between those channels. Another key ingredient, the local coupling phases of GEs, not only leads to asymmetric interference relations for oppositely propagating modes, but also provides the necessary degree of freedom for tuning the emission directions. Our setup can be a building block for generalized cascaded quantum networks with "correlated flying qubits", enabling numerous applications that are not accounted for in a linear cascaded interface.

Our work demonstrates an example of how correlated emission is significantly modified by the interplay of giant atoms and the bath nonlinearity. We believe it offers perspectives for harnessing many-body states, and thus provides a powerful toolbox for quantum-enhanced metrology, quantum information processing, and simulations[16–20].

Methods

Numerical simulation

To check the validity of the theoretical results in this study, we perform numerical simulations by considering an open-boundary waveguide with length $N = 3000$ in real space. In the two-excitation subspace, the dimension of this Hilbert space is approximately $N_H \simeq N^2/2 = 5\times10^6$. The numerical simulations of quantum dynamics are based on the open-source Python package QuTiP[83,84], which agrees well with theoretical results throughout our work.

Nonlinear cascaded master equation

We demonstrate how to derive the nonlinear cascaded master equation using the example of doublons serving as "flying qubits". Specifically, the evolution governed by the interaction Hamiltonian in Eq. (18) is derived as follows:

$$\begin{aligned}\dot{\rho} = &-\frac{i}{\hbar}\mathrm{Tr}_R\left[H_{\mathrm{int}}(t), \rho(t)\right]\\ &-\frac{1}{\hbar^2}\mathrm{Tr}_R\int_{t_0}^{t} dt'\left[H_{\mathrm{int}}(t), \left[H_{\mathrm{int}}(t'), \rho_S(t')\otimes\rho_R\right]\right],\end{aligned} \tag{25}$$

where ρ_S (ρ_R) denotes the density matrix of the emitters (nonlinear waveguide). The correlation relations for a doublon in the waveguide satisfy $\langle\mathcal{D}_K\rangle = \langle\mathcal{D}_K^\dagger\rangle = \langle\mathcal{D}_K^\dagger\mathcal{D}_K\rangle = 0$ and $\langle\mathcal{D}_K\mathcal{D}_K^\dagger\rangle = 1$. Then, we obtain

$$\dot{\rho} = -\int_{t_0}^{t} dt'\sum_{\alpha,\beta}\mathscr{A}_{\alpha,\beta}\left[-S_\beta^-\rho_S(t')S_\alpha^+ + S_\alpha^+S_\beta^-\rho_S(t')\right] + \mathrm{H.c.}, \tag{26}$$

where the coefficient is

$$\mathscr{A}_{\alpha,\beta} = \frac{g_\alpha^{*2}g_\beta^2}{J^2}\frac{1}{N_c}\sum_K F_{K,\alpha}^* F_{K,\beta}e^{-i\Delta_K(t-t')}. \tag{27}$$

Since only the modes centered around K_r are excited with high probability, the summation over K can be approximated as

$$\begin{aligned}&\sum_K F_{K,\alpha}^* F_{K,\beta}e^{-i\Delta_K(t-t')}\\ &\simeq \tfrac{N_c}{2\pi}F_{K_r,\alpha}^*F_{K_r,\beta}\int_{-\pi}^{\pi} dK\, e^{-i(K-K_r)v_g\left(t-t'-\frac{n_\alpha-n_\beta}{v_g}\right)}\\ &= \tfrac{N_c}{v_g}F_{K_r,\beta}^*F_{K_r,\alpha}\delta\left(t-t'-\tfrac{\Delta x_c}{v_g}\right),\end{aligned} \tag{28}$$

where $\Delta x_c/v_g = (n_\alpha - n_\beta)/v_g$ is the time delay between the two pairs, corresponding to the propagation time between pairs A and B with $n_{\alpha/\beta} = \left(n_{\alpha/\beta,1}^{r} - n_{\alpha/\beta,1}^{l}\right)/2$ being the positions of GEPs α/β. By employing the properties of the δ function,

$$\int_{t_0}^{t} dt'\delta\left(t-t'-\frac{\Delta x_c}{v_g}\right)\rho_S(t') = \begin{cases}0 & \Delta x_c/v_g < 0,\\ \frac{1}{2}\rho_S(t) & \Delta x_c/v_g = 0,\\ \rho_S(t) & \Delta x_c/v_g > 0,\end{cases} \tag{29}$$

the coefficients are written as ($n_A < n_B$)

$$\mathscr{A}_{\alpha,\alpha} = \frac{1}{2}\frac{g_\alpha^4}{J^2 v_g}\sum_{\pm}|F_{\pm K_r,\alpha}|^2 = \frac{\Gamma_+^\alpha + \Gamma_-^\alpha}{2}, \quad \alpha = \mathrm{A/B}, \tag{30}$$

$$\mathscr{A}_{\mathrm{A,B}} = \frac{g_\alpha^{*2}g_\beta^2}{J^2 v_g}F_{-K_r,\mathrm{A}}^*F_{-K_r,\mathrm{B}} = \Gamma_-^{\mathrm{AB}}, \tag{31}$$

$$\mathscr{A}_{\mathrm{B,A}} = \frac{g_\alpha^2 g_\beta^{*2}}{J^2 v_g}F_{+K_r,\mathrm{B}}^*F_{+K_r,\mathrm{A}} = \Gamma_+^{\mathrm{BA}}, \tag{32}$$

where we neglect the time-retardation effects by assuming $\rho(t - \Delta x_c/v_g) \approx \rho(t)$, and $\Gamma_\pm^\alpha$ correspond to the decay rates into the right- and left-propagating modes, respectively.

Finally, the master equation is

$$\begin{aligned}\dot{\rho} \;=\; & -\sum_{\alpha=\mathrm{A/B}} \frac{\Gamma_+^\alpha+\Gamma_-^\alpha}{2}\left[-S_\alpha^-\rho_S(t)S_\alpha^+ + S_\alpha^- S_\alpha^+\rho_S(t)\right] \\ & -\Gamma_+^{\mathrm{BA}}\left[-S_\mathrm{A}^-\rho_S(t)S_\mathrm{B}^+ + S_\mathrm{B}^+ S_\mathrm{A}^-\rho_S(t)\right] \\ & -\Gamma_-^{\mathrm{AB}}\left[-S_\mathrm{B}^-\rho_S(t)S_\mathrm{A}^+ + S_\mathrm{A}^+ S_\mathrm{B}^-\rho_S(t)\right] + \mathrm{H.c.}\end{aligned} \tag{33}$$

Note that $S_\mathrm{A}^- = \sigma_{\mathrm{A},1}^-\sigma_{\mathrm{A},2}^-$ ($S_\mathrm{B}^- = \sigma_{\mathrm{B},1}^-\sigma_{\mathrm{B},2}^-$) are joint-quantum-jump operators describing the two emitters in GEP A (B) simultaneously jumping to their ground states. Given that the two GEPs only interact with right-propagating modes, i.e., $\Gamma_+^\alpha \gg \Gamma_-^\alpha \simeq 0$, the master equation can be written as

$$\dot{\rho} = -i\left(H_\mathrm{eff}\rho - \rho H_\mathrm{eff}^\dagger\right) + \mathcal{L}\rho\mathcal{L}^\dagger, \tag{34}$$

$$H_\mathrm{eff} = -i\sum_{\alpha=\mathrm{A,B}} \frac{\Gamma_+^\alpha}{2} S_\alpha^+ S_\alpha^- - i\sqrt{\Gamma_+^\mathrm{A}\Gamma_+^\mathrm{B}}\, S_\mathrm{B}^+ S_\mathrm{A}^-, \tag{35}$$

$$\mathcal{L} = \sqrt{\Gamma_+^\mathrm{A}}S_\mathrm{A}^- + \sqrt{\Gamma_+^\mathrm{B}}S_\mathrm{B}^-. \tag{36}$$

where we have used the relation $\Gamma_+^{\mathrm{BA}} = \sqrt{\Gamma_+^\mathrm{A}\Gamma_+^\mathrm{B}}$. The second term of H_eff is unique to the cascaded system. It describes the process where a correlated photon pair is initially radiated by GEP A and subsequently absorbed by the other emitter pair without back-scattering.

Data availability

Supplementary data for all the figures are provided at https://doi.org/10.5281/zenodo.18409019. Additional data that support the findings of this study are available from the authors upon request.

Code availability

The codes used for the simulation and analysis of the data are available from the authors upon request.

Received: 2 July 2025; Accepted: 26 March 2026;
Published online: 13 April 2026

References

1. Cirac, J. I., Zoller, P., Kimble, H. J. & Mabuchi, H. Quantum state transfer and entanglement distribution among distant nodes in a quantum network. *Phys. Rev. Lett.* **78**, 3221–3224 (1997).
2. Mitsch, R., Sayrin, C., Albrecht, B., Schneeweiss, P. & Rauschenbeutel, A. Quantum state-controlled directional spontaneous emission of photons into a nanophotonic waveguide. *Nat. Commun.* **5**, 5713 (2014).
3. Pichler, H., Ramos, T., Daley, A. J. & Zoller, P. Quantum optics of chiral spin networks. *Phys. Rev. A* **91**, 042116 (2015).
4. Lodahl, P. et al. Chiral quantum optics. *Nature* **541**, 473 (2017).
5. De Bernardis, D., Piccioli, F. S., Rabl, P. & Carusotto, I. Chiral quantum optics in the bulk of photonic quantum hall systems. *PRX Quantum* **4**, 030306 (2023).
6. Guimond, P.-O. et al. A unidirectional on-chip photonic interface for superconducting circuits. *npj Quantum Inf.* **6**, 32 (2020).
7. Kannan, B. et al. On-demand directional microwave photon emission using waveguide quantum electrodynamics. *Nat. Phys.* **19**, 394 (2023).
8. Yao, W., Liu, R.-B. & Sham, L. J. Theory of control of the spin-photon interface for quantum networks. *Phys. Rev. Lett.* **95**, 030504 (2005).
9. Stannigel, K., Rabl, P., Sørensen, A. S., Lukin, M. D. & Zoller, P. Optomechanical transducers for quantum-information processing. *Phys. Rev. A* **84**, 042341 (2011).
10. Stannigel, K., Rabl, P. & Zoller, P. Driven-dissipative preparation of entangled states in cascaded quantum-optical networks. *N. J. Phys.* **14**, 063014 (2012).
11. Vermersch, B., Guimond, P.-O., Pichler, H. & Zoller, P. Quantum state transfer via noisy photonic and phononic waveguides. *Phys. Rev. Lett.* **118**, 133601 (2017).
12. Xiang, Z.-L., Zhang, M., Jiang, L. & Rabl, P. Intracity quantum communication via thermal microwave networks. *Phys. Rev. X* **7**, 011035 (2017).
13. Chang, D. E., Vuletic, V. & Lukin, M. D. Quantum nonlinear optics–photon by photon. *Nat. Photonics* **8**, 685 (2014).
14. Mahmoodian, S. et al. Strongly correlated photon transport in waveguide quantum electrodynamics with weakly coupled emitters. *Phys. Rev. Lett.* **121**, 143601 (2018).
15. Solano, P., Barberis-Blostein, P. & Sinha, K. Dissimilar collective decay and directional emission from two quantum emitters. *Phys. Rev. A* **107**, 023723 (2023).
16. Nagata, T., Okamoto, R., O'Brien, J. L., Sasaki, K. & Takeuchi, S. Beating the standard quantum limit with four-entangled photons. *Science* **316**, 726 (2007).
17. Yuan, Z.-S. et al. Entangled photons and quantum communication. *Phys. Rep.* **497**, 1–40 (2010).
18. Giovannetti, V., Lloyd, S. & Maccone, L. Advances in quantum metrology. *Nat. Photonics* **5**, 222 (2011).
19. Gatto Monticone, D. et al. Beating the abbe diffraction limit in confocal microscopy via nonclassical photon statistics. *Phys. Rev. Lett.* **113**, 143602 (2014).
20. Paulisch, V., Perarnau-Llobet, M., González-Tudela, A. & Cirac, J. I. Quantum metrology with one-dimensional superradiant photonic states. *Phys. Rev. A* **99**, 043807 (2019).
21. Sheremet, A. S., Petrov, M. I., Iorsh, I. V., Poshakinskiy, A. V. & Poddubny, A. N. Waveguide quantum electrodynamics: collective radiance and photon-photon correlations. *Rev. Mod. Phys.* **95**, 015002 (2023).
22. Mahmoodian, S., Calajó, G., Chang, D. E., Hammerer, K. & Sørensen, A. S. Dynamics of many-body photon bound states in chiral waveguide QED. *Phys. Rev. X* **10**, 031011 (2020).
23. Peyronel, T. et al. Quantum nonlinear optics with single photons enabled by strongly interacting atoms. *Nature* **488**, 57 (2012).
24. Roy, D., Wilson, C. M. & Firstenberg, O. Colloquium: strongly interacting photons in one-dimensional continuum. *Rev. Mod. Phys.* **89**, 021001 (2017).
25. Koch, J. et al. Charge-insensitive qubit design derived from the Cooper pair box. *Phys. Rev. A* **76**, 042319 (2007).
26. Orell, T., Michailidis, A. A., Serbyn, M. & Silveri, M. Probing the many-body localization phase transition with superconducting circuits. *Phys. Rev. B* **100**, 134504 (2019).
27. Blais, A., Grimsmo, A. L., Girvin, S. M. & Wallraff, A. Circuit quantum electrodynamics. *Rev. Mod. Phys.* **93**, 025005 (2021).
28. Lukin, M. D. et al. Dipole blockade and quantum information processing in mesoscopic atomic ensembles. *Phys. Rev. Lett.* **87**, 037901 (2001).
29. Gorshkov, A. V., Otterbach, J., Fleischhauer, M., Pohl, T. & Lukin, M. D. Photon-photon interactions via Rydberg blockade. *Phys. Rev. Lett.* **107**, 133602 (2011).
30. Fedorov, G. P. et al. Photon transport in a Bose-Hubbard chain of superconducting artificial atoms. *Phys. Rev. Lett.* **126**, 180503 (2021).
31. Karamlou, A. H. et al. Probing entanglement in a 2D hard-core Bose–Hubbard lattice. *Nature* **629**, 561 (2024).
32. Castillo-Moreno, C. et al. Experimental observation of multimode quantum phase transitions in a superconducting Bose-Hubbard simulator. Preprint at *arXiv* https://doi.org/10.48550/arXiv.2508.20116 (2025).
33. Weckesser, P. et al. Realization of a Rydberg-dressed extended Bose-Hubbard model. *Science* **390**, 849–853 (2025).

34. Winkler, K. et al. Repulsively bound atom pairs in an optical lattice. *Nature* **441**, 853 (2006).
35. Piil, R. & Mølmer, K. Tunneling couplings in discrete lattices, single-particle band structure, and eigenstates of interacting atom pairs. *Phys. Rev. A* **76**, 023607 (2007).
36. Valiente, M. & Petrosyan, D. Two-particle states in the Hubbard model. *J. Phys. B* **41**, 161002 (2008).
37. Mansikkamäki, O., Laine, S., Piltonen, A. & Silveri, M. Beyond hard-core bosons in transmon arrays. *PRX Quantum* **3**, 040314 (2022).
38. Wang, Z., Jaako, T., Kirton, P. & Rabl, P. Supercorrelated radiance in nonlinear photonic waveguides. *Phys. Rev. Lett.* **124**, 213601 (2020).
39. Talukdar, J. & Blume, D. Two emitters coupled to a bath with Kerr-like nonlinearity: exponential decay, fractional populations, and Rabi oscillations. *Phys. Rev. A* **105**, 063501 (2022).
40. Li, J.-Q. & Wang, X. Environmental quantum states trigger emission in nonlinear photonics. *Commun. Phys.* **8**, 511 (2025).
41. Zhang, X., Guo, X., Zhang, Y., Wang, X. & Wang, Z. Quantum state preparation and transfer based on the bound state in the doublon continuum. Preprint at *arXiv* https://doi.org/10.48550/arXiv.2512.01339 (2025).
42. Rieck, W., Kockum, A. F. & Chen, G. Doublon bound states in the continuum through giant atoms. Preprint at *arXiv* https://doi.org/10.48550/arXiv.2511.18212 (2025).
43. Frisk Kockum, A., Delsing, P. & Johansson, G. Designing frequency-dependent relaxation rates and Lamb shifts for a giant artificial atom. *Phys. Rev. A* **90**, 013837 (2014).
44. Frisk Kockum, A. *Quantum Optics with Giant Atoms—the First Five Years*, 125–146 (Springer Singapore, 2020). https://doi.org/10.1007/978-981-15-5191-8_12.
45. Du, L., Zhang, Y., Wu, J.-H., Kockum, A. F. & Li, Y. Giant atoms in a synthetic frequency dimension. *Phys. Rev. Lett.* **128**, 223602 (2022).
46. Terradas-Briansó, S., González-Gutiérrez, C. A., Nori, F., Martín-Moreno, L. & Zueco, D. Ultrastrong waveguide QED with giant atoms. *Phys. Rev. A* **106**, 063717 (2022).
47. Qiu, Q.-Y., Wu, Y. & Lü, X.-Y. Collective radiance of giant atoms in non-Markovian regime. *Sci. China Phys. Mech*. https://doi.org/10.1007/s11433-022-1990-x (2023).
48. Gustafsson, M. V. et al. Propagating phonons coupled to an artificial atom. *Science* **346**, 207 (2014).
49. Aref, T. et al. Quantum acoustics with surface acoustic waves. In (eds Hadfield, R. H. & Johansson, G.) *Superconducting Devices in Quantum Optics* (Springer, 2016).
50. Guo, L., Grimsmo, A., Kockum, A. F., Pletyukhov, M. & Johansson, G. Giant acoustic atom: a single quantum system with a deterministic time delay. *Phys. Rev. A* **95**, 053821 (2017).
51. Andersson, G., Suri, B., Guo, L., Aref, T. & Delsing, P. Non-exponential decay of a giant artificial atom. *Nat. Phys.* **15**, 1123 (2019).
52. Vadiraj, A. M. et al. Engineering the level structure of a giant artificial atom in waveguide quantum electrodynamics. *Phys. Rev. A* **103**, 023710 (2021).
53. Wang, X. & Li, H.-R. Chiral quantum network with giant atoms. *Quantum Sci. Technol.* **7**, 035007 (2022).
54. Wang, Z.-Q. et al. Giant spin ensembles in waveguide magnonics. *Nat. Commun.* **13**, 7580 (2022).
55. Kockum, A. F., Johansson, G. & Nori, F. Decoherence-free interaction between giant atoms in waveguide quantum electrodynamics. *Phys. Rev. Lett.* **120**, 140404 (2018).
56. Kannan, B. et al. Waveguide quantum electrodynamics with superconducting artificial giant atoms. *Nature* **583**, 775 (2020).
57. Carollo, A., Cilluffo, D. & Ciccarello, F. Mechanism of decoherence-free coupling between giant atoms. *Phys. Rev. Res.* **2**, 043184 (2020).
58. Soro, A., Muñoz, C. S. & Kockum, A. F. Interaction between giant atoms in a one-dimensional structured environment. *Phys. Rev. A* **107**, 013710 (2023).
59. Guo, L., Kockum, A. F., Marquardt, F. & Johansson, G. Oscillating bound states for a giant atom. *Phys. Rev. Res.* **2**, 043014 (2020).
60. Noachtar, D. D., Knörzer, J. & Jonsson, R. H. Nonperturbative treatment of giant atoms using chain transformations. *Phys. Rev. A* **106**, 013702 (2022).
61. Lim, K. H., Mok, W. K. & Kwek, L. C. Oscillating bound states in non-Markovian photonic lattices. *Phys. Rev. A* **107**, 023716 (2023).
62. Zhao, W. & Wang, Z. Single-photon scattering and bound states in an atom-waveguide system with two or multiple coupling points. *Phys. Rev. A* **101**, 053855 (2020).
63. González-Tudela, A., Muñoz, C. S. & Cirac, J. I. Engineering and harnessing giant atoms in high-dimensional baths: a proposal for implementation with cold atoms. *Phys. Rev. Lett.* **122**, 203603 (2019).
64. Wang, X., Liu, T., Kockum, A. F., Li, H.-R. & Nori, F. Tunable chiral bound states with giant atoms. *Phys. Rev. Lett.* **126**, 043602 (2021).
65. Joshi, C., Yang, F. & Mirhosseini, M. Resonance fluorescence of a chiral artificial atom. *Phys. Rev. X* **13**, 021039 (2023).
66. Scully, M. O. & Zubairy, M. S. *Quantum Optics* (Cambridge University Press, 1997).
67. Ramos, T., Vermersch, B., Hauke, P., Pichler, H. & Zoller, P. Non-Markovian dynamics in chiral quantum networks with spins and photons. *Phys. Rev. A* **93**, 062104 (2016).
68. Wang, X., Zhu, H.-B., Liu, T. & Nori, F. Realizing quantum optics in structured environments with giant atoms. *Phys. Rev. Res.* **6**, 013279 (2024).
69. Gao, Z.-M., Li, J.-Q., Wu, Y.-H., Liu, W.-X. & Wang, X. Harnessing spontaneous emission of correlated photon pairs from ladder-type giant atoms. *Phys. Rev. A* **110**, 053706 (2024).
70. Wang, D.-W., Zhu, S.-Y., Evers, J. & Scully, M. O. High-frequency light reflector via low-frequency light control. *Phys. Rev. A* **91**, 011801 (2015).
71. Zhong, Y. et al. Deterministic multi-qubit entanglement in a quantum network. *Nature* **590**, 571–575 (2021).
72. Strand, H. U. R., Eckstein, M. & Werner, P. Beyond the Hubbard bands in strongly correlated lattice bosons. *Phys. Rev. A* **92**, 063602 (2015).
73. Sajna, A. S. Effects of higher-order energy bands and temperature on the bosonic Mott insulator in a periodically modulated lattice. *Phys. Rev. A* **94**, 043612 (2016).
74. Chang, C. W. S. et al. Observation of three-photon spontaneous parametric down-conversion in a superconducting parametric cavity. *Phys. Rev. X* **10**, 011011 (2020).
75. Gu, X., Kockum, A. F., Miranowicz, A., Liu, Y.-X. & Nori, F. Microwave photonics with superconducting quantum circuits. *Phys. Rep.* **718-719**, 1 (2017).
76. Krantz, P. et al. A quantum engineer's guide to superconducting qubits. *Appl. Phys. Rev.* **6**, 021318 (2019).
77. Hacohen-Gourgy, S., Ramasesh, V. V., De Grandi, C., Siddiqi, I. & Girvin, S. M. Cooling and autonomous feedback in a Bose-Hubbard chain with attractive interactions. *Phys. Rev. Lett.* **115**, 240501 (2015).
78. Roushan, P. et al. Spectroscopic signatures of localization with interacting photons in superconducting qubits. *Science* **358**, 1175–1179 (2017).
79. Kim, E. et al. Quantum electrodynamics in a topological waveguide. *Phys. Rev. X* **11**, 011015 (2021).
80. Roushan, P. et al. Chiral ground-state currents of interacting photons in a synthetic magnetic field. *Nat. Phys.* **13**, 146 (2017).
81. Krinner, S. et al. Realizing repeated quantum error correction in a distance-three surface code. *Nature* **605**, 669 (2022).
82. Place, A. P. M. et al. New material platform for superconducting transmon qubits with coherence times exceeding 0.3 milliseconds. *Nat. Commun.* **12**, 1779 (2021).
83. Johansson, J. R., Nation, P. D. & Nori, F. QuTiP: an open-source Python framework for the dynamics of open quantum systems. *Comput. Phys. Commun.* **183**, 1760 (2012).

84. Johansson, J. R., Nation, P. D. & Nori, F. QuTiP 2: a Python framework for the dynamics of open quantum systems. *Comput. Phys. Commun.* **184**, 1234 (2013).

Acknowledgements
X.W. is supported by the National Natural Science Foundation of China (NSFC) (Grant No. 12174303). Z.H.W. acknowledges the support from the National Natural Science Foundation of China (Grant No. 12375010). T.L. acknowledges the support from Guangdong Provincial Quantum Science Strategic Initiative (Grant No. GDZX2505004), National Natural Science Foundation of China (Grant No. 12274142), and the Introduced Innovative Team Project of Guangdong Pearl River Talents Program (Grant No. 2021ZT09Z109). A.F.K. acknowledges support from the Swedish Research Council (grant number 2019-03696), the Swedish Foundation for Strategic Research (grants numbers FFL21-0279 and FUS21-0063), the Horizon Europe program HORIZON-CL4-2022-QUANTUM-01-SGA via the project 101113946 OpenSuperQPlus100, and from the Knut and Alice Wallenberg Foundation through the Wallenberg Centre for Quantum Technology (WACQT). F.N. is supported in part by the Japan Science and Technology Agency (JST) [via the CREST Quantum Frontiers program Grant No. JPMJCR24I2, the Quantum Leap Flagship Program (Q-LEAP), the Moonshot R&D Grant Number JPMJMS256E, and the ASPIRE program (Grant Number JPMJAP2513).

Author contributions
X.W. and T.L. conceived the original idea. J.Q.L. did the analytical and numerical analysis under the supervision of X.W. and T.L. Z.H.W., A.F.K., L.D., and F.N. provided very useful insights and guidance. All authors contributed to and approved the final version of the paper.

Competing interests
The authors declare no competing interests.

Additional information
Supplementary information The online version contains supplementary material available at https://doi.org/10.1038/s42005-026-02618-3.

Correspondence and requests for materials should be addressed to Xin Wang or Tao Liu.

Peer review information *Communications Physics* thanks the anonymous reviewers for their contribution to the peer review of this work. A peer review file is available.